Organometalliclike localization of 4d-derived spins in an inorganic conducting niobium suboxide

K.-W. Lee[1,2,*] and W. E. Pickett[3,†]

[1]*Department of Applied Physics, Graduate School, Korea University, Sejong 339-700, Korea*

[2]*Department of Display and Semiconductor Physics, Korea University, Sejong 339-700, Korea*

[3]*Department of Physics, University of California, Davis, California 95616, USA*

Based on the refined crystal structure comprised of columns of 3×4 planar blocks of NbO_6 octahedra and first principles electronic structure methods, we find that orthorhombic (o)-$Nb_{12}O_{29}$ introduces a new class of transition metal oxide. The electronic system consists of a large Nb dimer-based localized orbital comparable in size to those in organometallic compounds, yet is tightly bound and weakly interacting with itinerant electronic bands. These local moments—a rare occurrence for Nb—form one-dimensional spin chains that criss-cross perpendicularly oriented conducting "nanowires." The local moment bandwidth is comparable to what is seen in rare earth compounds with extremely localized orbitals. The microscopic origin is traced to the local structure of the NbO_6 octahedra and associated orbital+spin ordering. The resulting $1D_s \times 1D_c$ anisotropic two dimensional Heisenberg-Kondo lattice model (s = spin; c = charge) provides a strongly anisotropic spin-fermion lattice system for further study.

I. INTRODUCTION

Transition metal oxides form some of the most intellectually rich electronic phases, viz. the high temperature superconducting cuprates, the colossal magnetoresistance manganites, and ordering of charge, spin, orbital, and structural changes, especially in 3d oxides. Niobates are 4d oxides that assume a fascinating sequence of crystal structures with assorted properties, extending from the cubic one-to-one, formally Nb^{2+}, metal NbO to the Nb^{5+}-based wide-gap insulator Nb_2O_5, and encompassing a sequence of mixed valent compounds such as $Nb_{12}O_{29}$, $Nb_{22}O_{54}$, $Nb_{25}O_{62}$, $Nb_{47}O_{116}$, and so on.

The 12-29 member, $Nb_{12}O_{29}$, displays local moment behavior coexisting with a relatively high density of conducting carriers [1]. Just how local moments—very rare for Nb—emerge and coexist with itinerant electrons in this system has remained an enigma for decades. More broadly, systems of local moments embedded in conducting media form a rich platform for unusual phases, with phenomena including Kondo systems, heavy fermion metals and superconductors, and still unexplained non-Fermi liquid behavior.

$Nb_{12}O_{29}$ originally attracted attention [2,3] due to the mixed valent character it implied for Nb: $2\,Nb^{4+} + 10\,Nb^{5+}$ balancing the oxygen charge, apparently leaving two Nb cations with $4d^1$ configuration. It lies just inside the line of conducting compounds in the Nb_2O_{5-2x} system, where coexistence of polarons and bipolarons had provided the prevailing picture of its conducting behavior [4,5]. The tungsten bronzes, which share the same underlying WO_3 structural motif, have been found to superconduct up to 4 K when heavily doped [6,7].

$Nb_{12}O_{29}$ is found in two polymorphs, orthorhombic (o-) and monoclinic ($m-$), both based on stacking of the same underlying structural feature (described below) but being stacked differently. The magnetic susceptibility of each polymorph displays Curie-Weiss susceptibility corresponding to one spin-half moment per f.u. [1]. m-$Nb_{12}O_{29}$ orders around 12 K, in the sense that the susceptibility follows a behavior that peaks before dropping, in a manner that can be fit by the Bonner-Fisher form for a one dimensional (1D) Heisenberg antiferromagnet [8]. o-$Nb_{12}O_{29}$ does not show such a peak down to 2 K [9].

This first (and still one of few) observation of Nb local moment behavior, moreover to be coexisting with Nb conductivity [1,5], suggested a more specific picture [1] of one d^1 electron becoming localized and magnetic while the other is itinerant and Pauli paramagnetic. While this compound is a very bad metal, it is nevertheless also a standout transparent conductor, displaying resistivity $\sim 3\,m\Omega\,cm$ with only 10% variation [1,10] from room temperature to 2 K, and it possesses a high carrier density [10] of one carrier per Nb thus not requiring tuning via extrinsic doping. Fang $et\ al.$ recently argued from a density functional study using the generalized gradient approximation (GGA) functional that the monoclinic polymorph is an itinerant Stoner magnet [11]. Our studies provide a very different picture of o-$Nb_{12}O_{29}$, and we contrast the two pictures below.

In this paper we demonstrate that orthorhombic o-$Nb_{12}O_{29}$ presents an unprecedented type of material, based on an unusual large but strongly localized and magnetic organometalliclike orbital [12]. This compound consists at the most basic level of an array of linear (1D) Heisenberg magnetic chains along the one direction, crisscrossed by 1D conducting nanowires along a perpendicular direction, coupled to a two dimensional (2D) system by Kondo interaction at each site. This new $1D \times 1D$ Heisenberg-Kondo lattice (HKL) system arises from the intricate structure of columns of 3×4 planar units of NbO_6 octahedra, with the spin-half *dimer Mott insulating system* arising from quantum confinement induced extreme localization on Nb *dimers* with a specific 4d orbital orientation, while other Nb sites provide electronic conduction. These results should stimulate further study both experimentally, to identify the very low temperature and high magnetic field phases, and theoretically to probe a new model system for novel magnetic and possibly exotic superconducting states,

*mckwan@korea.ac.kr

†pickett@physics.ucdavis.edu

since related 2D models have been shown to harbor pairing correlations.

II. STRUCTURE AND APPROACH

$Nb_{12}O_{29}$ assumes two polymorphs, monoclinic (*m-*) [8,9,13–16] and orthorhombic (*o-*) [1,9,13]. Each is based on the same 3×4 block structure of corner-linked NbO_6 octahedra (ReO_3-type perovskite) that are stacked along the $\hat{a}$ direction with lattice constant $a = 3.832$ Å, thus forming rectangular $\infty \times 3 \times 4$ nanocolumns (in $\hat{a}, \hat{b}, \hat{c}$ order of the Nb sites). The 3×4 blocks contain six crystallographic sites Nb1,..., Nb6. The two structures differ only in how these columns are repeated in the $\hat{b} - \hat{c}$ plane, a common motif in polymorphic shear structures.

We focus here on o-$Nb_{12}O_{29}$ [1,9,13] with $b = 20.740$ Å, $c = 28.890$ Å, whose crystal structure was only settled by use of x-ray diffraction together with convergent beam electron diffraction on single crystals by McQueen *et al.* [13]. The structure at 200 K, shown in Fig. 1, has centered orthorhombic space group *Cmcm* (no. 63) with two f.u. per primitive cell. The primitive cell consists of two such columns, one of which lies $\frac{a}{2}$ lower/higher than the other, so these two NbO_6 columns are connected edgewise rather than corner-linked. These shear boundaries, we find, severely limit carrier hopping in the $\hat{b} - \hat{c}$ plane. Due to the distortion of the Nb-O bond lengths and angles, the 3×4 unit is ferroelectric in symmetry. The centering+reflection symmetry operation however results in no net electric polarization in the cell.

Density functional theory (DFT) calculations were carried out initially using the spin-polarized Perdew-Burke-Ernzerhof GGA functional [17], implemented in an all-electron full-potential code FPLO [18]. The on-site Coulomb repulsion U was treated within the the GGA+U approach [19,20]. We present results for $U = 3$ eV, the value calculated [21] for Nb in perovskite $SrNbO_3$, and Hund's energy $J^H = 1$ eV;
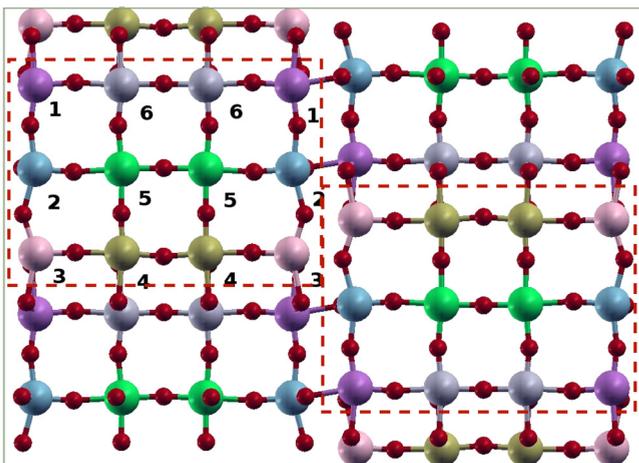

FIG. 1. (Color online) View of the structure in the $\hat{c} - \hat{b}$ plane ($\hat{c}$ horizontal) of o-$Nb_{12}O_{29}$. The designations of the sites Nb1, Nb2,..., Nb6 in the 3×4 unit are indicated. The dashed lines outline two of the 3×4 units that lie on the same level. Other such units (only partially visible) lie at a height $\frac{a}{2}$ along $\hat{a}$. Note that the (green) Nb5 site is the only one not on a "surface" of the 3×4 unit.

we verified that results are insensitive to the specific values. A similar value of U has been applied in the DFT plus dynamical mean field method to study the dynamical excitation spectrum of $Li_{1-x}NbO_2$ [22], which as one of the few strongly correlated niobates has become of interest because as a strongly layered transition metal oxide it becomes superconducting, thus displaying several similarities to the high temperature superconducting cuprates. The Brillouin zone was sampled with a regular fine mesh up to 657 irreducible k points.

III. THEORETICAL PICTURE

A. Electronic configuration

We first address the electronic structure before consideration of magnetism. The system was earlier found to be too intricate for Hückel methods to elucidate [23]. The atom-projected density of states (PDOS) in Fig. 2 reveals a sharp and narrow Nb5-dominated peak, with secondary contribution from Nb4 and Nb6, that pins the Fermi level E_F and will be found to be unstable to local moment formation. Itinerant band states around E_F are dominated by the Nb2 site, with smaller Nb3 participation but *none* from Nb5. The band structure in Fig. 3 reveals a $Nb5_2$ *dimer bonding band* lying within the continuum of $\hat{a}$-axis dispersive conduction bands, with remarkable flat-band dispersion of no more than 75 meV along each of the three axes. The antibonding partner lies $\sim$2.8 eV higher and is bifurcated by additional interactions. From the small dispersion of the flat Nb5 band, we obtain the nearest neighbor hopping amplitudes along the three axes: $t_5^a \approx -10$ meV, $t_5^b = 17$ meV, and $t_5^c = 0$. (The dispersion along $\hat{a}$ is however not simple nearest neighbor type, in spite of the small value.)

The anomalously flat band arises primarily from the Nb5 d_{yz} orbital, which significantly has its lobes lying in the $\hat{b} - \hat{c}$ plane, perpendicular to the column $\hat{a}$ direction. This orientation provides only a tiny $dd\delta$ overlap (t_5^a above) for hopping along the short $\hat{a}$ axis. The hopping amplitudes given above are orders of magnitude smaller than the on-site Coulomb repulsion that will produce Mott localization of d_{yz} states on the $Nb5_2$ dimer. The two neighboring Nb5 d_{yz} orbitals form bonding-antibonding combinations by strong $dd\pi$ coupling, splitting the molecular orbitals by $2t_{5,\pi} = 2.8$ eV. The $Nb5_2$ dimer bonding combination ϕ_b is partially filled and pins E_F.

The Nb2-derived conducting "wires," a pair on opposing columnar faces perpendicular to $\hat{c}$ and two columns per primitive cell, lead to four bands that disperse through E_F along $(k_a,0,0)$. Coupling between the conducting wires lifts the degeneracy, as can be seen from the occupied bands along Γ-X in Figs. 3 and 4. Only two bands cross E_F along Γ-Y. There are four flat, 1D sheets perpendicular to $\hat{a}$, plus some small and probably unimportant sheets. These flat sheets, with wave vectors $k_F \approx \pm(0.15 - 0.35)\frac{\pi}{a}$, imply large susceptibilities and impending intracolumnar 1D instabilities at several Fermi surface nesting calipers. The several different nesting wave vectors that connect the various 1D FS sheets will however tend to frustrate any specific instability (viz. charge or spin density waves, or Peierls distortions).
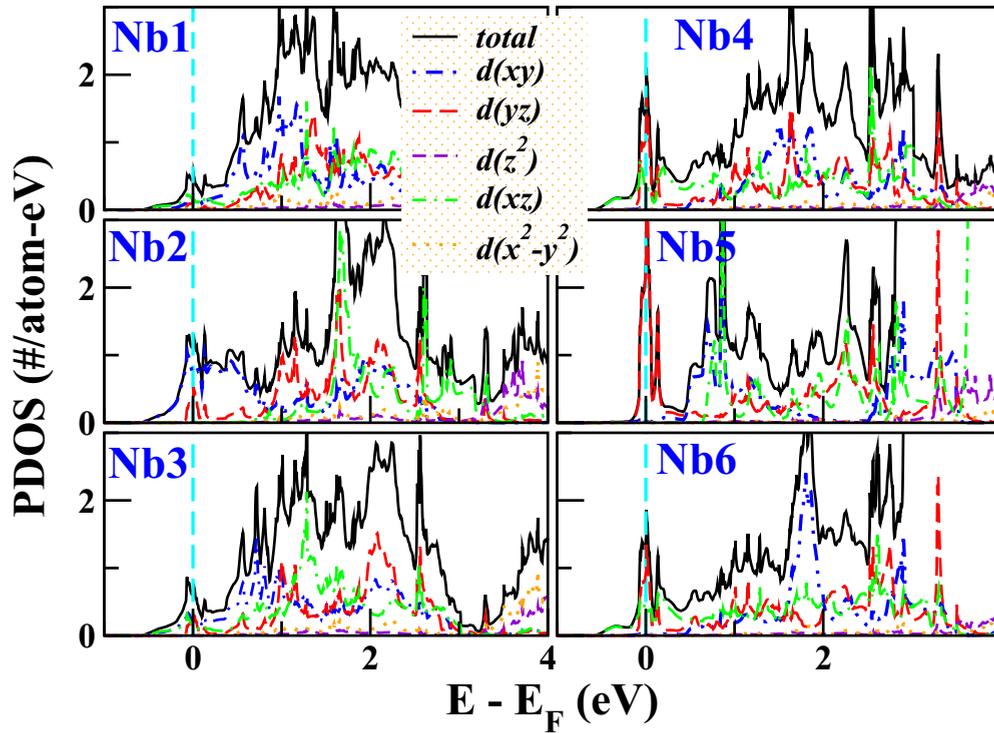
FIG. 2. (Color online) Total and orbital-projected density of states for each of the Nb sites in nonmagnetic $Nb_{12}O_{29}$. Note that Nb5 dominates the peak at the Fermi level E_F, while Nb2 dominates the occupied states at and below E_F.

B. Magnetic character

The conventional GGA treatment of electronic exchange and correlation processes produces a Slater magnetic moment arising from the exchange-split flat band. However, in flat-band transition metal oxides such as this (though rarely as extreme), explicit attention to on-site repulsion is important, so we focus on the GGA+U treatment [19,20] that is often successful in treating strong interaction effects. Here U is the Hubbard repulsion on the Nb ions supplementing the semilocal GGA exchange-correlation potential [17].

From the correlated treatment, one peculiar feature is that the magnetic moment arises from a single electron on the $Nb5_2$ *dimer* rather than on a single atom. This distinction makes it a quarter-filled band system that results in a dimer Mott insulating (dMI) subsystem [24], a phase not yet reported in otherwise conducting 3D systems. Dimer Mott insulators are
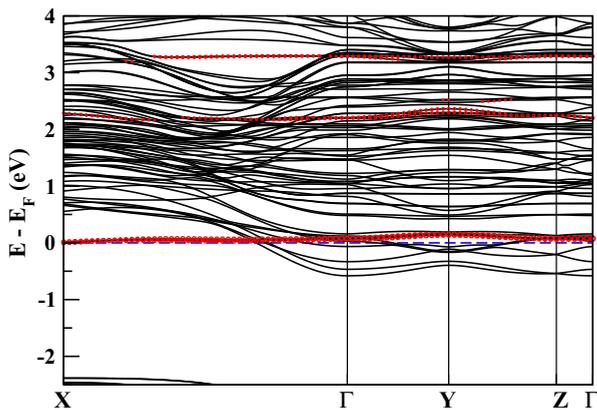

FIG. 4. (Color online) Fatband plots of the bands of $Nb_{12}O_{29}$ near E_F, without and with the strong interaction (U). The magnetic bands within GGA (left panel) highlight the flat Nb5 d_{yz} band; the dispersive bands within ±0.6 eV of E_F are strongly Nb2 d_{xy}-derived. The right panel shows the bands from a ferromagnetic GGA+U calculation, with lower Hubbard band in red. The upper Hubbard band lies above this energy window. The splitting of majority (minority) conduction bands [yellow (green)], $\sim$40 meV near E_F, provides a measure of the Kondo coupling of the spins to the itinerant electrons.

FIG. 3. (Color online) Full band region of nonmagnetic $Nb_{12}O_{29}$, above the gap separating them from the O $2p$ bands. The red horizontal lines indicate a single, remarkably flat, d_{yz} bonding and (split apart) antibonding band pair of the $Nb5_2$ dimer. Symmetry points are $X = (\frac{\pi}{a},0,0)$, $Y = (0,\frac{\pi}{b},0)$, and $Z = (0,0,\frac{\pi}{c})$.
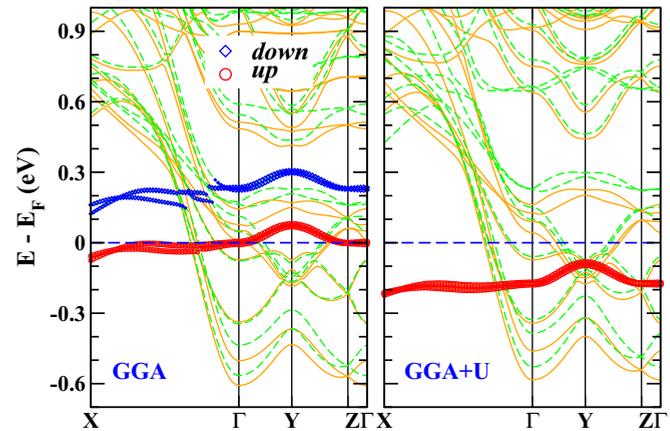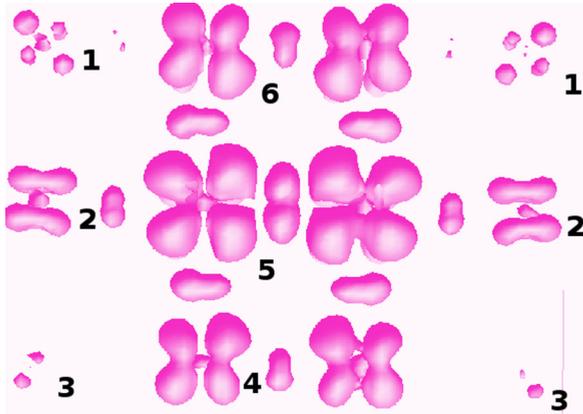
FIG. 5. (Color online) $Nb5_2$-centered spin density isosurface, looking down on one layer of the 3×4 unit in the $\hat{b} - \hat{c}$ plane, of the magnetic electron in $Nb_{12}O_{29}$. Since the state is weakly mixed in all three directions, the spin density is also the density of the corresponding $Nb5_2$ dimer centered molecular orbital ϕ_b. A majority of the density lies on the central $Nb5_2$ dimer d_{yz} orbitals and the intervening O p_y orbital.

FIG. 6. (Color online) Schematic representation of the active states in $Nb_{12}O_{29}$. Spin chains (arrows) form columns along $\hat{a}$ but are coupled most strongly along $\hat{b}$ (hence shown antialigned), while they are uncoupled along $\hat{c}$. Each spin is positioned between two "wires" conducting along the $\hat{a}$ axis; the green shading gives an idea of the conduction electron density spread.

rare, although a *trimer* Mott insulator has been reported [25]. The $Nb5_2$ dimer orbital density $|\phi_b|^2$, also the spin density, is displayed in Fig. 5, and its bonding character (incorporating the intervening O ion) is evident.

This dMI occupied state however lies within the continuum of occupied conduction bands. From the nearly invisible band mixing with the conduction bands (see Fig. 4), it is found that band mixing (charge coupling) with the conduction electrons is quite small. Then, from the splitting of majority and minority conduction bands (see Fig. 4) the exchange (Kondo) coupling along $\hat{b}$, $J_K \vec{s}_j \cdot \vec{S}_j$, between itinerant $\vec{s}_j$ and localized $\vec{S}_j$ spins at site j, has coupling strength $J_K = 20$ meV that reproduces the spin splitting of the conduction bands in Fig. 4 for ferromagnetic alignment.

Three features may be contributing to the special behavior of the Nb5 site. First, quantum confinement: Nb5 is the only site interior to the 3×4 block; it is not an interface atom. Second, its octahedron is much more regular than for the other sites, having only a single Nb5-O distance [13] greater than 2.00 Å. Third, the anisotropic displacement parameter (U_{11} describing displacement from the ideal position in the $\hat{a}$ direction) is six times larger than for any other Nb site, reflecting dynamic (or possibly spatial) fluctuations in position.

$Nb_{12}O_{29}$ thus presents a novel type of system with interacting local moments in a conducting background—a Heisenberg-Kondo lattice system. The earlier 1D HKL model has been generalized to two dimensions in a maximally anisotropic matter: spin coupling in one direction and fermion hopping in the perpendicular direction. The basic picture is illustrated schematically in Fig. 6. Geometrically, the picture is one of 1D Heisenberg spin chains of $Nb5_2$ local moments extending along $\hat{b}$, sandwiched between nanowires (or "tapes") conducting along $\hat{a}$, lying on the faces of the columns perpendicular to $\hat{b}$. The lack of dispersion along $\hat{c}$ can be ascribed both to the electronic disruption caused by the shear boundaries, and to the centering+mirror symmetry operation
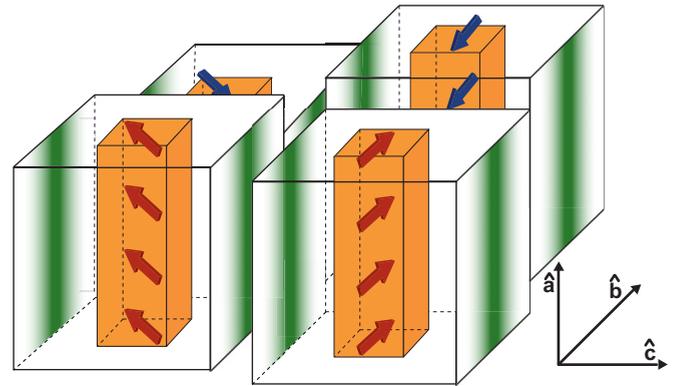
that serves to produce maximum separation of neighboring Nb sites.

This picture of o-$Nb_{12}O_{29}$ differs from that of m-$Nb_{12}O_{29}$ presented by Fang *et al.* [11]. Based on GGA alone and the VASP code, they presented a picture of a weak itinerant (Stoner) moment arising from a flat band with magnetic exchange splitting of 0.3 eV. This result is much like what we obtained for o-$Nb_{12}O_{29}$ at the GGA level (see Fig. 4). Our view is that the flat band requires consideration of correlation effects. Several specific differences follow, viz. strong local moment leading to a dMI subsystem versus a spin-split band Stoner moment in a fully itinerant system, and the corresponding coupling to the carriers. Such differences can be resolved by more extensive experimental study at low temperature.

IV. DISCUSSION

From the hopping amplitudes given above, the largest magnetic coupling is not along the structural $\hat{a}$ chain, but rather between neighboring $Nb5_2$ pairs in the $\hat{b}$ direction, corresponding to a superexchange coupling through the oxide ions at the edges of the 3×4 blocks of $J_H = 4(t_5^b)^2/U \sim 0.5$ meV $= 6$ K. We presume the direct exchange will be smaller, based on the molecular orbital pictured in Fig. 5, because the direct overlap with neighboring orbitals seems very minor. The moments will be relatively uncorrelated along the conducting $\hat{a}$ direction ($J^a \sim 2$ K), with the dominant antiferromagnetic (AFM) correlations developing along $\hat{b}$ only at low temperature below J^b. This temperature scale is roughly consistent with that from susceptibility $\chi(T)$ [9], which shows spin-half behavior with $\theta_{CW} = -14$ K, but no deviation from Curie-Weiss behavior down to 2 K. The monoclinic phase, which we will address elsewhere, "orders" via displaying a χ peak at 12 K that can be fit [8] with the Bonner-Fisher form [26] for the 1D Heisenberg chain (which shows no true long-range order).

The basic Hamiltonian to model such a system, neglecting band indices and spin chain indices for the simplest model, is

$$H = -t \sum_{j,\alpha} [c^{\dagger}_{j,\alpha} c_{j+\hat{a},\alpha} + c^{\dagger}_{j,\alpha} c_{j-\hat{a},\alpha}]$$
$$+ J_H \sum_j \vec{S}_j \cdot \vec{S}_{j+\hat{b}} + J_K \sum_j \vec{s}_j \cdot \vec{S}_j, \qquad (1)$$

where j,α run over the 2D lattice and spin directions, $\hat{a}$ and $\hat{b}$ are the 2D lattice vectors, $\vec{\sigma}$ is the Pauli spin matrix vector, and $\sum_{\alpha\beta} c^{\dagger}_{j,\alpha} \vec{\sigma}_{\alpha\beta} c_{j,\beta} = \vec{s}_j$ is the conduction electron spin at site j in terms of the carrier creation operator $c^{\dagger}_{j\sigma}$. The energy scales are $t = 400$ meV, $J_H \approx 0.5$ meV, and $J_K = 20$ meV. In this model an itinerant electron is confined to its nanowire, and suffers only Kondo (spin) scattering due to the interaction. The 1D Heisenberg chains likewise are perturbed only by spin coupling to itinerant electrons.

The strictly 1D version of the Heisenberg-Kondo lattice model has been studied actively [27,28] in the context of high temperature superconducting cuprates, where 1D structures with entwined charge, spin, and superconducting orders have been detected experimentally. The 2D HKL model has recently been applied to model behavior, and pairing symmetry, in heavy fermion superconductors [29–31]. This new $1D_c \times 1D_s$ model of coupled 1D charge (c) wires and 1D spin (s) chains comprises a type of system with frustrating interactions. 1D conductors have thoroughly studied charge- and spin-density wave instabilities at $2k_F$ and $4k_F$, respectively. Are these instabilities overcome by the Kondo coupling, which results in coupled 1D conductors and hence a 2D system? The AFM ordering tendencies of the Heisenberg chain, which never actually attains long range order, are correlated with neighboring chains by the Kondo coupling. A plausible mean field picture might be that Heisenberg spin chains coupled, either in phase or out of phase, with neighboring spins chains by the Kondo coupling through the conducting wires. The corresponding spin-exchange and magnetic ordering could introduce superstructure into the fermionic susceptibility at commensurate wave vectors, possibly influencing the diverging susceptibility at $2k_F$ on the conducting systems, through the induced alternating "magnetic field" transferred through the Kondo coupling. This system may lead to a new form of magnetic polarons, accounting for the bad conductor behavior that is so prominent in low carrier density transition metal oxides. Superconducting pairing tendencies become an attractive possibility, due to the analogies with cuprates; note that $Nb_{12}O_{29}$ is a magnetic 2D transition metal oxide with $\sim$0.1 carrier per metal ion. We expect that low temperature and high field studies of this system could reveal unusual transport, thermodynamic, and spectroscopic behavior.

V. SUMMARY

In this electronic structure study of o-$Nb_{12}O_{29}$, two remarkable features have been uncovered. First, regardless of whether strong on-site interaction effects are included in the calculation, a remarkably flat Nb 4*d* band is found to exist within bands of several itinerant (dispersive) Nb 4*d* bands. Secondly, when correlation effects are included, the majority spin component of this flat band state is fully occupied, but the orbital is shared by two Nb sites, the Nb5 sites interior to the 3 × 4 columnar array of NbO_6 octahedra. The itinerant, conducting states are found to reside along the edges of the columns, forming 1D wires. The magnetic spins are (i) coupled to neighboring spins along a single direction, and (ii) coupled to the itinerant carriers by Kondo coupling. This combination appears to be quite delicate: while the orthorhombic polytype that we have studied does not order down to 2K, the monoclinic polytype with many structural similarities "orders" in the sense of a 1D Heisenberg chain, with the susceptibility following the Bonner-Fisher form.

The picture of $Nb_{12}O_{29}$ that arises makes more explicit the earlier picture of "one magnetic Nb ion and one conducting Nb ion." A local moment does emerge as required by the susceptibility data, but it is a highly unusual *dimer moment* rather than a single ion moment. Similarly, the conducting state arises not from a single Nb ion providing an itinerant electron; instead the conducting electron is shared between two conducting "wires" on either edge of the 3 × 4 columns of NbO_6 octahedra. The novel state that results is an illustration of how structural complexity can give rise to new emergent phases of matter. This new understanding of this Nb suboxide should serve to guide study of the more complex Nb suboxides mentioned in the Introduction.

[1] R. J. Cava, B. Batlogg, J. J. Krajewski, P. Gammel, H. F. Poulsen, W. F. Peck, Jr., and L. W. Rupp, Antiferromagnetism and metallic conductivity in $Nb_{12}O_{29}$, Nature (London) **350**, 598 (1991).

[2] S. Iijima, Ordering of point-defects in nonstoichiometric crystals of $Nb_{12}O_{29}$, Acta Crystallogr., A **31**, 784 (1975).

[3] B. Meyer and R. Gruen, Beiträge zur untersuchung anorganischer nichtstöchiometrischer verbindungen. XIV. oxydationsprodukte von orthorhombischem $Nb_{12}O_{29}$ elektronenoptische Untersuchung, Z. Anorg. Allg. Chem. **484**, 77 (1982).

[4] C. H. Rüscher, E. Salje, and A. Hussian, The effect of high polaron concentration on the polaron transport in $NbO_{2.5-x}$: optical and electrical properties, J. Phys. C **21**, 3737 (1988).

[5] C. H. Rüscher and M. Nygren, Magnetic properties of phases possessing block type structures in the Nb_2O_{5-2x} system, with $0 \leqslant x \leqslant 0.083$, J. Phys.: Condens. Matter **3**, 3997 (1991).

[6] A. R. Sweedler, J. K. Hulm, B. T. Matthias, and T. H. Geballe, Superconductivity of barium tungsten bronze, Phys. Lett. **19**, 82 (1965).

[7] N. Haldolaarachchige, Q. Gibson, J. Krisan, and R. J. Cava, Superconducting properties of the $K_x WO_3$ tetragonal tungsten bronze and the superconducting phase diagram of the tungsten bronze family, Phys. Rev. B **89**, 104520 (2014).

[8] A. Lappas, J. E. L. Waldron, M. A. Green, and K. Prassides, Magnetic ordering in the charge-ordered $Nb_{12}O_{29}$, Phys. Rev. B **65**, 134405 (2002).

[9] E. N. Andersen, T. Klimczuk, V. L. Miller, H. W. Zandbergen, and R. J. Cava, Nanometer structural columns and frustration of magnetic ordering in $Nb_{12}O_{29}$, Phys. Rev. B **72**, 033413 (2005).

[10] T. Ohsawa, J. Okubo, T. Suzuki, H. Kumigashira, M. Oshima, and T. Hitosugi, An n-type transparent conducting oxide: $Nb_{12}O_{29}$, J. Phys. Chem. C **115**, 16625 (2011).

[11] C. M. Fang, M. A. van Huis, Q. Xu, R. J. Cava, and H. W. Zandbergen, Unexpected origin of magnetism in monoclinic $Nb_{12}O_{29}$ from first-principles calculations, J. Mater. Chem. C **3**, 651 (2015).

[12] V. V. Maslyuk, A. Bagrets, V. Meded, A. Arnold, F. Evers, M. Brandbyge, T. Bredow, and I. Mertig, Organometallic benzene-vanadium wire: A one-dimensional half-metallic ferromagnet, Phys. Rev. Lett. **97**, 097201 (2006).

[13] T. McQueen, Q. Xu, E. N. Andersen, H. W. Zandbergen, and R. J. Cava, Structures of the reduced niobium oxides $Nb_{12}O_{29}$ and $Nb_{22}O_{54}$, J. Solid State Chem. **180**, 2864 (2007).

[14] J. E. L. Waldron, M. A. Green, and D. A. Neumann, Charge and spin ordering in monoclinic $Nb_{12}O_{29}$, J. Am. Chem. Soc. **123**, 5833 (2001).

[15] J. E. L. Waldron, M. A. Green, and D. A. Neumann, Structure and electronic properties of monoclinic $Nb_{12}O_{29}$, J. Phys. Chem. Solids **65**, 79 (2004).

[16] J.-G. Cheng, J.-S. Zhou, J. B. Goodenough, H. D. Zhou, C. R. Wiebe, T. Takami, and T. Fujii, Spin fluctuations in the antiferromagnetic metal $Nb_{12}O_{29}$, Phys. Rev. B **80**, 134428 (2009).

[17] J. P. Perdew, K. Burke, and M. Ernzerhof, Generalized gradient approximation made simple, Phys. Rev. Lett. **77**, 3865 (1996).

[18] K. Koepernik and H. Eschrig, Full-potential nonorthogonal local-orbital minimum-basis band-structure scheme, Phys. Rev. B **59**, 1743 (1999).

[19] V. I. Anisimov, F. Aryasetiawan, and A. I. Lichtenstein, First-principles calculations of the electronic structure and spectra of strongly correlated systems: the LDA+U method, J. Phys.: Condens. Matter **9**, 767 (1997).

[20] E. R. Ylvisaker, K. Koepernik, and W. E. Pickett, Anisotropy and magnetism in the LSDA+U method, Phys. Rev. B **79**, 035103 (2009).

[21] L. Baugier, H. Jiang, and S. Biermann, Hubbard U and Hund exchange J in transition metal oxides: Screening versus localization trends from constrained random phase approximation, Phys. Rev. B **86**, 165105 (2012).

[22] K.-W. Lee, J. Kunes, R. T. Scalettar, and W. E. Pickett, Correlation effects in the triangular lattice single-band system $Li_x NbO_2$, Phys. Rev. B **76**, 144513 (2007).

[23] M. Llunell, P. Alemany, and E. Canadell, Crystal structure and coexistence of localized and delocalized electrons in $Nb_{12}O_{29}$, J. Solid State Chem. **149**, 176 (2000).

[24] H. Seo, C. Hotta, and H. Fukuhama, Toward systematic understanding of diversity of electronic properties in low-dimensional molecular solids, Chem. Rev. **104**, 5005 (2004).

[25] V. Pardo and W. E. Pickett, Quantum confinement induced molecular mott insulating state in $La_4 Ni_3 O_8$, Phys. Rev. Lett. **105**, 266402 (2010).

[26] J. C. Bonner and M. E. Fisher, Linear magnetic chains with anisotropic coupling, Phys. Rev. **135**, A640 (1964).

[27] O. Zachar, S. A. Kivelson, and V. J. Emery, Exact results for a 1D Kondo lattice from bosonization, Phys. Rev. Lett. **77**, 1342 (1996).

[28] E. Berg, E. Fradkin, and S. A. Kivelson, Pair-density-wave correlations in the kondo-heisenberg model, Phys. Rev. Lett. **105**, 146403 (2010).

[29] N. K. Sato, N. Aso, K. Miyake, R. Shiina, P. Thalmeier, G. Varelogiannis, C. Geibel, F. Steglich, P. Fulde, and T. Komatsubara, Strong coupling between local moments and superconducting 'heavy' electrons in $UPd_2 Al_3$, Nature (London) **410**, 340 (2001).

[30] J. C. Xavier and E. Dagotto, Robust d-wave pairing correlations in the heisenberg kondo lattice model, Phys. Rev. Lett. **100**, 146403 (2008).

[31] Y. Liu, G.-M. Zhang, and L. Yu, Pairing symmetry of heavy fermion superconductivity in the two dimensional Kondo-Heisenberg lattice model, Chin. Phys. Lett. **31**, 087102 (2014).